The prediction of liquid film journal bearing performance with a consideration of lubricant film reformation Part 2: experimental results

D Dowson, BSc, PhD, DSc, CEng, FIMechE and **C M Taylor,** BSc(Eng), MSc, CEng, MIMechE
The Institute of Tribology, Department of Mechanical Engineering, University of Leeds

A A S Miranda, MSc, PhD
University of Minho, Braga, Portugal

Analyses and design data for plain journal bearings rarely take into account the phenomenon of film reformation. The consideration of the re-establishment of the lubricant film after the cavitation region is difficult in a number of ways. The importance of allowing for reformation is, however, being increasingly recognized. This is particularly true as regards the satisfactory prediction of lubricant flowrate and the thermal operating characteristics of a bearing. The authors have previously implemented a cavitation algorithm to enable the cavitation region in a plain journal bearing to be located automatically and efficiently in a computer analysis. In Part 1 of the present paper theoretical results have been presented for the case of a plain bearing with a square-ended, axial groove located at the position of maximum film thickness. The second part of the paper gives details of an experimental investigation designed to establish the validity of the analysis.

NOTATION

a	groove width
b	bearing width
c	radial clearance
c_d	diametral clearance
d	shaft diameter $[=2r]$
e	eccentricity
p_f	supply pressure
$\bar{p}_f$	dimensionless supply pressure $[=p_f(c/r)^2/\eta\Omega]$
Q_s	side leakage flowrate
$\bar{Q}_s$	dimensionless side leakage flowrate $[=Q_s/cbU]$
t	temperature
U	shaft surface velocity $[=r\Omega]$
w	groove (circumferential) length
α_c	rupture boundary location
α_r	reformation boundary location
ε	eccentricity ratio $[=e/c]$
η	dynamic viscosity
ν	kinematic viscosity
Ω	angular velocity

1 INTRODUCTION

The authors have previously published details of their implementation of the cavitation algorithm of Elrod and Adams (**2, 3**) to enable the rupture and reformation boundaries in a plain journal bearing to be located efficiently by numerical analysis (**1**). In Part 1 of the present paper theoretical results for a wide range of operating parameters were presented for the case of a full 360° bearing with a single, square-ended, axial groove located at the maximum film thickness position. In Part 2 of the paper an experimental study to investigate the correlation between the theoretical predictions and empirical data is described.

The test facility developed had the specific aim of making precise measurements of the lubricant flowrate and of the location of the rupture and reformation boundaries. Through the use of glass bushes a visualization of the flow in each bearing was possible. The design of the apparatus enabled the eccentricity ratio to be fixed for a given test, while shaft rotational speed and lubricant supply pressure could be varied. The experimental results were compared not only against the authors' own predictions but also with the data presented in ESDU Item No. 66023 (**4**). The latter design document has been discussed in Part 1 of the paper.

2 EXPERIMENTAL APPARATUS AND INSTRUMENTATION

2.1 The apparatus

A photograph of the experimental apparatus is shown in Fig. 1. A brief description of its construction, the test bearings and associated instrumentation will be given; fuller details may be found in Miranda (**5**).

The test machine consisted essentially of two brackets, one fixed and supporting the main shaft assembly, the other movable and carrying the glass bush mounting device. The position of the movable bracket with respect to the fixed one was controlled by the thicknesses of an interchangeable packing plate and a pair of interchangeable packing blocks. By this means a preselected operating eccentricity ratio for the test bearing could be precisely set.

The steel test shaft was mounted on taper roller bearings preloaded to remove internal clearance and to increase stiffness. The preloading system consisted of six helical springs, each having a spring constant of 93 kN/m, the preload being transmitted to the test bearing

The MS was received on 29 June 1984 and was accepted for publication on 16 October 1984.

0263-7154/85 $2.00 + .05

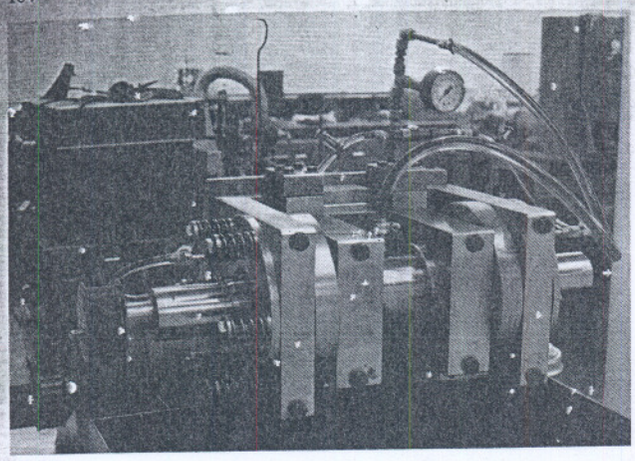

Fig. 1 The test apparatus

through an end cap. The shaft was driven through a pulley system by an infinitely variable speed, 1.1 kW electric motor. The test bush was mounted on brass clamp sleeves. These were pulled against the tapered ends of the glass bushes by means of six clamping screws, three on each side, 120° apart. In addition six adjustment screws were provided to assist in the setting of the test bushes.

Glass bushes were used in the experiments. Their bores showed a maximum departure from circularity of 18 μm, compared with the radial clearance to be employed in the bearings of 138 μm. Three bushes were used in the experiments the dimensions of which, apart from the geometry of the oil supply recess, were not significantly different. Two of the test bushes are shown in Fig. 2. The wall thickness of the bushes was approximately 6.5 mm and the dimensions of each are detailed in Fig. 3. As can be seen bush 1 had a supply hole whilst the remaining two bushes had grooves to introduce the lubricant into the clearance space. The diameter of the oil inlet pipe to all the bushes was 6 mm. The technique used to machine the supply grooving has been fully documented (**5**). Careful calculations were carried out to determine the deformation of the glass bushes when subjected to the most adverse of the test conditions contemplated. The changes in film shape due to such deflections were insignificant.

The lubricant supply system consisted of a supply tank containing about twelve litres of oil, a pump with a

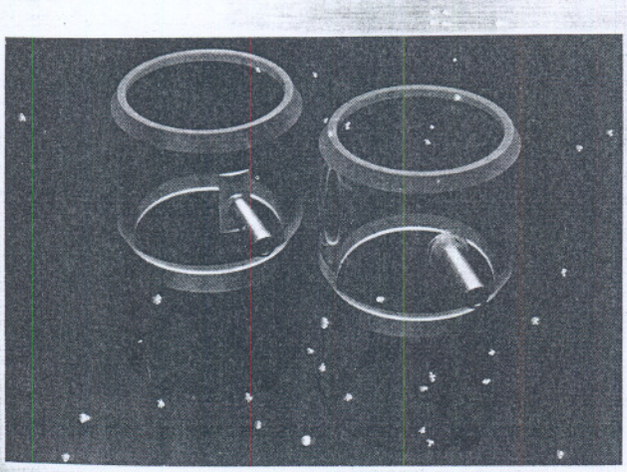

Fig. 2 Two glass test bushes

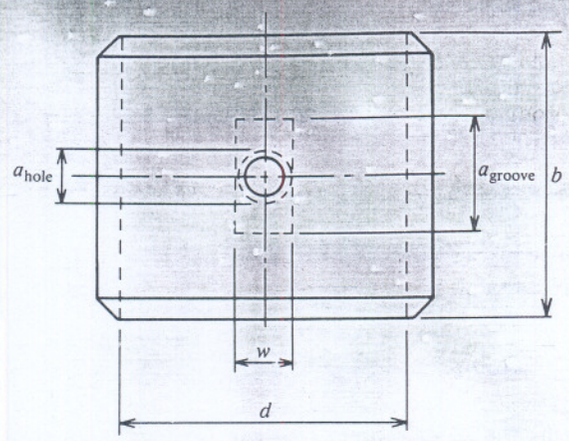

	Supply geometry					Resulting C_d
Bush 1	Oil hole	63·50(1)	63·5	12	12	0·27 (6)
Bush 2	Axial groove	63·50(2)	63·5	26	12	0·27 (7)
Bush 3	Axial groove	63·50(2)	63·5	45	12	0·27 (6)

Fig. 3 Dimensions in mm of the glass bushes used in the experimental programme. Shaft diameter 63.22(5) mm

variable speed drive, a relief valve and pulsation damper. The oil issuing from the bearing was discharged into a collecting tray and returned by gravity to the supply tank. The variable speed drive fitted to the pump enabled the oil supply pressure to the test bearing to be altered. At supply pressures greater than 1.5–2.0 bar (150–200 kN/m^2) it was found necessary to incorporate a damper in the supply system in order to smooth the pulsations in oil flow delivered by the pump. The damper consisted of a rubber sleeve, through which the lubricant passed, housed in a chamber supplied with air under pressure. The lubricant employed was a Shell oil designated HVI 60, a straight mineral oil to which a red dye was added to facilitate visual observations of the oil film in the bearing. A suspended level U-tube capillary viscometer was used to determine the viscosity characteristics of the lubricant. The kinematic viscosity (v in centistokes) of the oil as a function of temperature (t in °C) was determined to be:

$$\log_{10} \log_{10}(v + 0.8) = 9.567 - 3.772 \log_{10}(t + 273)$$

The density of the lubricant at 19°C was 867.5 kg/m^3 and variations of density with temperature over the conditions of the experiments were not significant. Thus the dynamic viscosity of the lubricant was 0.0224 Ns/m^2 at 40°C and 0.004 Ns/m^2 at 100°C.

2.2 The instrumentation

Provision was made to enable the accurate determination of the following parameters.

(a) *Eccentricity ratio* By design the value of the eccentricity ratio and the location of the position of maximum film thickness were to be determined by the

thickness of the packing blocks and plate mentioned in Section 2.1. In fact this did not prove entirely reliable due to the flexibility of the components involved. A reproducible technique of setting a preselected value of eccentricity ratio was therefore developed (**5**). The most suitable packing blocks for a design value of eccentricity ratio were first assembled in the test apparatus. The actual eccentricity ratio was then determined by use of a dial gauge. The gauge was attached to the inlet brass pipe of the test bush by means of an adapter sleeve. The plunger of the indicator passed through the inlet pipe and groove to contact the shaft directly. When the glass bush was rotated by hand about the stationary shaft the position of maximum clearance and the eccentricity ratio could be determined by the displacement of the plunger as indicated on the dial gauge. The approach of setting the eccentricity ratio greatly facilitated the comparison of theoretical and experimental results, since without a precise measurement of it such a correlation would become questionable. The disadvantage of the arrangement adopted was that the load on the bearing was not known directly. However, for the purpose of the test programme proposed this was not an inconvenience.

(b) *Shaft rotational speed* This was determined using a hand tachometer.

(c) *Lubricant supply pressure* A Bourdon-tube pressure gauge was used to measure the pressure of the oil supplied to the test bearing. A flexible plastic pipe 9 mm in diameter and 0.8 m long connected the point where the pressure gauge was positioned (see Fig. 1) with the bush inlet pipe. The pressure drop down this pipe was negligibly small compared with the magnitudes of supply pressures adopted.

(d) *Lubricant temperatures* For this purpose nickel–chromium/nickel–aluminium thermocouples in conjunction with an electronic thermometer were employed. An iced water bath was used to check the thermometer reference zero temperature. The temperature of the oil inlet to the bush and side leakage from the bush were measured directly. The temperature rise of the lubricant as it passed through the test bush was small enough to justify the use of the lubricant outlet temperature as the effective operating temperature. No direct measurements of temperature in the lubricant film were made (**5**).

(e) *Lubricant flowrate* The method used to measure the side leakage rate from a test bearing was simple and rendered reliable, reproducible results. The oil discharged from the sides of the test bearing during a given time interval of a particular test was collected in a portable tray the weight of which had previously been determined. The tray and oil collected were then weighed and the flowrate determined with a knowledge of the density of the lubricant.

(f) *Location of the rupture and reformation boundaries* A scale graduated in degrees was engraved on one of the brass clamp sleeves holding the glass test bush. This enabled adequate determination of the location of the rupture and reformation boundaries on the bearing centre-line and edge with respect to the oil inlet, which was located at the maximum film thickness position.

Extensive commissioning tests were carried out to identify the potential sources of discrepancy between the theoretical and experimental data (**5**). The results of such tests confirmed that the apparatus could be used with confidence to provide experimental data for a wide range of operating parameters. A careful test procedure was developed and this has been described in detail by Miranda (**5**). It is worthy of note that thermal stabilization of the apparatus for a particular set of test conditions took about four hours. Fortunately, the rate of change of the lubricant temperatures as measured was moderate and it proved unnecessary to wait for stabilization before taking results. Changes over the time period necessary to effect all measurements required were small and could be accommodated by a simple averaging procedure.

3 THE TEST PROGRAMME AND SOME QUALITATIVE OBSERVATIONS

The dimensionless groups pertinent to the analysis described in Part 1 of the paper were b/d, a/b, w/d, ε and $\bar{p}_f$. For the three bushes used in the experiments (see Fig. 1), the groups defining the bearing and groove geometry were as follows:

Bush number	Supply geometry	Bearing width to diameter ratio b/d	Groove to bearing width ratio a/b	Groove length to bearing diameter ratio w/d
Bush 1	Oil hole	1	0.189	0.189
Bush 2	Axial groove	1	0.409	0.189
Bush 3	Axial groove	1	0.709	0.189

The radial clearance ratio, c/r, was 4.37×10^{-3} for each bearing. The parameters which could be varied in the tests were eccentricity ratio, ε, and dimensionless supply pressure, $\bar{p}_f$. The latter group was dependent upon oil supply pressure, shaft speed and the effective temperature (or viscosity) of the lubricant; the first two of these were fixed while the latter was measured.

Two basic sets of experiments were carried out as indicated in Fig. 4. In the first of these each of the three bushes was tested at the same fixed shaft speed for a complete permutation of six values of eccentricity ratio between 0.2–0.8 and four values of gauge supply pressure from zero to 2.7 bar (0–270 kN/m^2). For the second set of experiments only bush 2 was tested. The eccentricity ratio was fixed and tests carried out for five shaft rotational frequencies from 200–1000 r/min at two values of oil supply pressure.

The use of glass bushes permitted visualization of the oil film in the bearing. The onset and physical nature of cavitation has proved to be of interest and fascination to many research workers. Some particular features observed by the authors were:

1. In the test carried out with bush 1 (oil hole) at low values of eccentricity ratio (<0.3) and at the fixed shaft rotational frequency of 600 r/min (10 Hz), a complete film of oil was observed around the bearing at all oil supply pressures tested. When the shaft speed was increased air bubbles eventually appeared in the divergent film region. The value of shaft speed at which this occurred was dependent upon the supply pressure and decreased as the latter increased.

	Bush involved	Eccentricity ratio	Oil supply pressure, bar (kN/m^2)		Journal speed, r/min (Hz)
Set of experiments 1	Bush 1	0·27	0	(0)	600 (10)
		0·44	0·68	(68)	
		0·57	1·7	(170)	
		0·67	2·7	(270)	
		0·74			
	Bush 2	0·26	0	(0)	600 (10)
		0·41	0·68	(68)	
		0·47	1·7	(170)	
		0·58	2·7	(270)	
		0·67			
		0·76			
	Bush 3	0·29	0	(0)	600 (10)
		0·38	0·68	(68)	
		0·47	1·7	(170)	
		0·58	2·7	(270)	
		0·67			
		0·74			
Set of experiments 2	Bush 2	0·67	0	(0)	200 (3·33)
			1·7	(170)	400 (6·66)
					600 (10)
					800 (13·33)
					1000 (16·66)

Fig. 4 The programme of tests

Some of the air forming these bubbles, which were not fixed in position, had been induced through the oil supply pipe and moved upstream on entry to the bearing film. In the experiments with bush 2 (axial groove, $a/b = 0.409$) at $\varepsilon = 0.26$ air bubbles appeared in the region upstream of the groove when the supply pressure was above ambient. At zero supply pressure there was a complete oil film. With bush 3 (axial groove, $a/b = 0.709$) at $\varepsilon = 0.29$ air bubbles were observed in the divergent film region at all supply pressures tested.

2. As the eccentricity ratio was increased for all tests the rupture and reformation boundaries could be clearly identified giving a well defined cavitation region. Any axial misalignment between bush and shaft could be detected by the lack of symmetry of the bubble pattern in the cavitation zone or more particularly by the shape of the reformation boundary. While the rupture boundary was more or less straight, the reformation boundary at either low or high supply pressure conditions had a curved shape very similar to that predicted by the theoretical analysis. Figure 5 shows experimentally observed reformation boundaries and the corresponding theoretical predictions for two different operating conditions.
3. The influence of the oil supply pressure on the extent of the complete width film was clearly seen in the tests involving bushes 1 and 2. At a given shaft speed and eccentricity ratio, and with zero gauge supply pressure, the cavitation region extended well downstream of the inlet. As the supply pressure increased

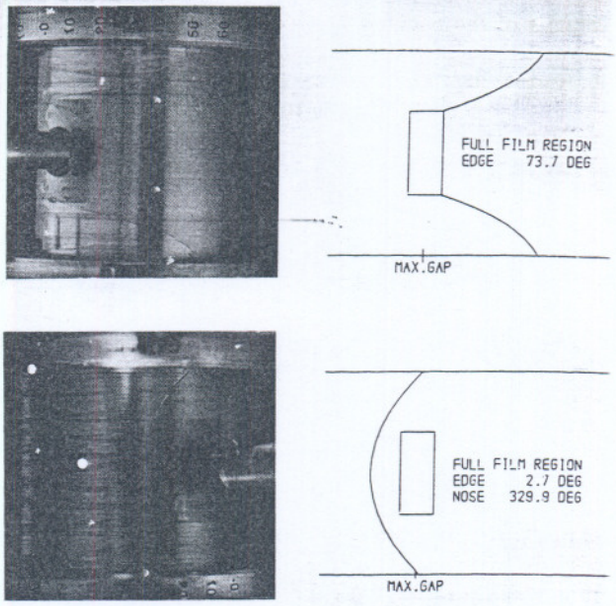

Fig. 5 The experimentally observed (left) and the theoretically predicted (right) shapes of the film reformation boundary for *bush 2* at $\varepsilon = 0.67$, $\bar{p}_f = 0$ (upper) and $\varepsilon = 0.67$, $\bar{p}_f = 0.64$ (lower). Shaft rotation was from left to right

the reformation boundary moved upstream. The location of the rupture boundary was not significantly affected by the oil supply pressure, an observation which is in agreement with theoretical predictions.

4. In tests with a variable shaft speed a stable reformation boundary was observed at low values of supply pressure. At higher values of supply pressure however, an instability was observed at the air–oil interface in the film reformation zone. This was characterized by the local breakdown of the air–oil interfaces due to what seemed to be the collapse of air bubbles carried by the oil inlet stream and moving upstream from the inlet to the reformation boundary. At given values of eccentricity ratio and oil supply pressure there existed a value of shaft speed above which this instability occurred. This phenomenon has also been observed by Cole and Hughes (**6**) and Hargreaves and Taylor (**7**).

4 RESULTS AND DISCUSSION

The empirical results obtained from the first set of experiments detailed in Figure 4 were designed to give data for a fixed shaft speed and variable eccentricity ratio and supply pressure. The most convenient way of presenting a comparison of experimental results and theoretical predictions was in a graphical form often with the dimensionless supply pressure $[\bar{p}_f = p_f(c/r)^2/\eta\Omega]$ as a parameter. Whilst the angular velocity Ω, and oil supply pressure, p_f, could be kept constant for fixed values of these quantities the dimensionless supply pressure varied from one eccentricity ratio situation to the next by virtue of the change in the temperature and hence dynamic viscosity, η. It proved convenient, therefore, to interpolate the results for the side leakage rate and the location of the rupture and

reformation boundaries, at selected values of dimensionless supply pressure, for each value of eccentricity ratio considered. The nature of the variation of these parameters was entirely conducive to such an interpolation. Values of the dimensionless supply pressure of 0, 0.5, 1.0, 1.5 were chosen for this process.

4.1 Side leakage flow

Figures 6 and 7 show the variation of the dimensionless side flowrate, $\bar{Q}_s$, with eccentricity ratio for the four values of the dimensionless oil supply pressure. The interpolated experimental results are compared with the theoretical predictions, based on the authors' film reformation analysis. Figure 6 is for bush 1 (oil hole supply) whilst Fig. 7 relates to the grooved bush 2. Excellent correlation between the experimental data and theoretical predictions has been achieved for both bushes, as indeed it was for bush 3, the corresponding results for which may be found in Miranda (**5**).

The theoretical results for bush 1 were obtained by taking a 'square' supply hole of side equal to the oil hole diameter. For this bush at $\bar{p}_f = 0.5$ the maximum percentage difference obtained between the interpolated experimental results and theoretical predictions was 17.2 per cent (percentage differences are with respect to the theoretical result). At other values of the dimensionless supply pressure the correlation was better, the maximum discrepancy at $\bar{p}_f = 1.5$ being 12.7 per cent.

With bush 2, as can be seen from Fig. 7, very good correlation of side flowrate was achieved at low values of the dimensionless supply pressure (0 and 0.5) for all values of eccentricity ratio. At higher values of $\bar{p}_f$ the experimental results began to show some scatter. However, the maximum percentage difference between the experimental and theoretical predictions was limited to 22.8 per cent at $\bar{p}_f = 1.5$. Many factors could be responsible for the discrepancy between the experimental data and theoretical predictions. Errors in the determination of eccentricity ratio and the location of the maximum film thickness position will be partially responsible, however, shaft/bush misalignment was thought to be a more significant factor. Deficiencies in the theoretical model must also be borne in mind when contemplating the differences. The discrepancies are remarkably low and the recognition of this fact is most important.

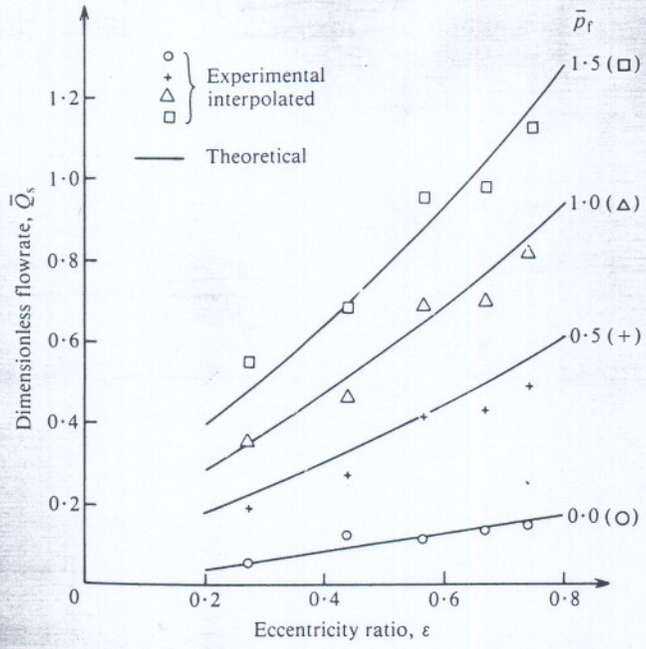

Fig. 6 A comparison of the interpolated experimental results of dimensionless side flowrate with the theoretical predictions for *bush 1* (oil hole). Rotational speed of the shaft 600 r/min (10 Hz)

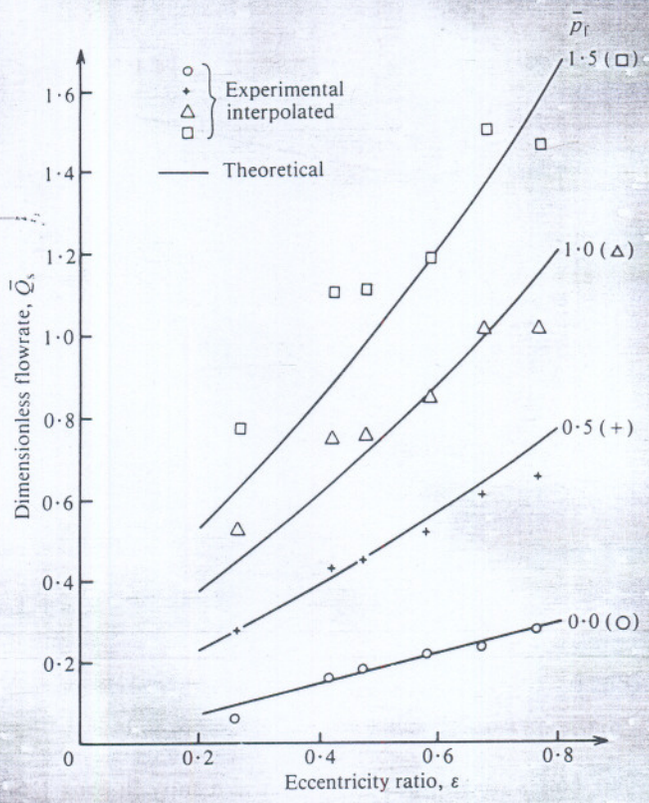

Fig. 7 A comparison of the interpolated experimental results of dimensionless side flowrate with the theoretical predictions for *bush 2* (axial groove, $a/b = 0.409$). Rotational speed of the shaft 600 r/min (10 Hz)

The effect of shaft rotational frequency on side flowrate for bush 2 is shown in Fig. 8. The dimensional results presented are for a fixed eccentricity ratio ($\varepsilon = 0.67$) and for two tests with gauge supply pressures of 0 and 1.7 bar. Once again excellent correlation between experimental results and theoretical predictions was obtained. At the supply pressure of 1.7 bar the experimental flowrates were all greater than the theoretical predictions, the maximum difference being 14.2 per cent at the lowest shaft speed.

When the differences between the side leakage rates for the two supply pressure situations shown in Fig. 8 are calculated, they are found to be in the range 13.5–14.2 $\times 10^{-6}$ m^3/s) for all values of shaft speed. This is an interesting observation which lends support to the approach adopted by a number of journal bearing design procedures in which side leakage is calculated as the sum of two components: (a) a 'zero supply pressure flow' in which flow is induced by the shaft surface speed and (b) a 'zero velocity flow' which depends upon the lubricant supply pressure and is determined assuming a stationary journal. For the case of the ESDU Item

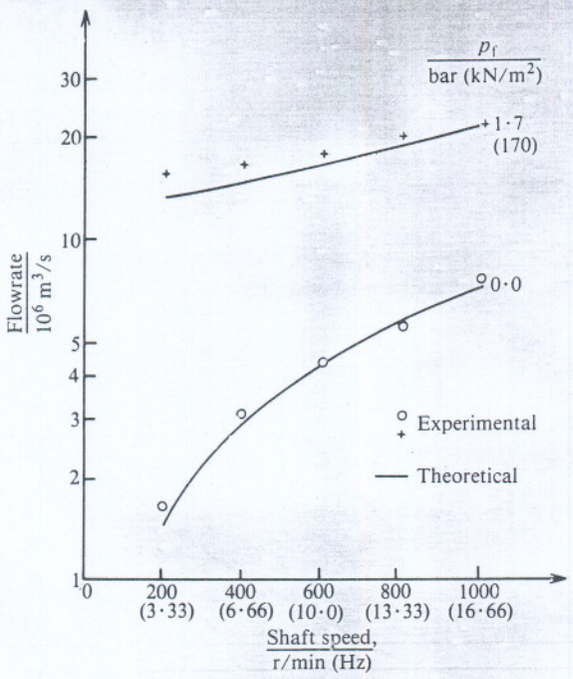

Fig. 8 The influence of shaft speed on side flowrate for *bush 2* (axial groove, $a/b = 0.049$) at fixed $\varepsilon = 0.67$

No. 66023 (**4**) this has been discussed fully in Part 1 of the paper.

In considering the agreement between experimentally measured and theoretically predicted flowrates obtained by the authors, it is important to put the results into the context of correlations often obtained. The lack of agreement is sometimes so profound that researchers choose not to make comparisons in their published work. Differences of over 100 per cent are not uncommon (**7**) and this has tended to cast doubt upon the data used in design procedures and their influence upon critical design parameters such as maximum bush temperature. Hargreaves and Taylor (**7**, **8**) in a study directed towards obtaining an improved understanding of the true lubricant flowrate in bearings and its satisfactory prediction examined a grooved, rectangular, thrust bearing. With careful attention to the design of the experimental apparatus and the elimination or reduction of the factors likely to cause a discrepancy between experimental measurements and theoretical predictions of flowrate, good agreement was obtained. For a static bearing (**8**) an average discrepancy of less than 7 per cent in 180 tests was obtained. With a moving runner (**7**), for which an air–lubricant interface akin to the reformation boundary in a journal bearing may occur, the error was 20 per cent over a series of 235 tests. Such results suggested that theoretical predictions of flowrate, with a sound model of the lubricant film and its cavitation interfaces, were adequate. The poor correlation often obtained might be due either to ill defined experimental conditions (e.g. undue misalignment) or an unsatisfactory model of the lubricant film.

The outstanding correlation obtained between theory and practice by the present authors for lubricant flowrate in a journal bearing matches the results of Hargreaves and Taylor for the grooved thrust bearing geometry. The carefully controlled experimental tests have resulted in empirical data which bears excellent comparison with the analytical predictions using the film reformation model. Such agreement would clearly have been much worse (see Part 1 of the paper) had the theoretical predictions been made on the basis of an analysis taking no reformation of the lubricant film into account.

4.2 The location of the film reformation and reformation boundaries

A comparison of the experimental measurements of the angular location of the beginning of the full width film, α_r, and the angular location of the film rupture boundary, α_c, with theoretical predictions was carried out for all the tests conducted. The correlation for all three test bushes was similar.

Figure 9 shows a comparison of the experimentally determined reformation boundary location, α_r, with theoretical predictions for bush 2 taking a fixed shaft speed. For all values of eccentricity ratio very good correlation was achieved at the larger values of dimensionless supply pressure (1.0 and 1.5). The maximum discrepancy for $\bar{p}_f = 1.5$ was 5°. While the agreement in observed and predicted locations of the reformation boundary was good at high eccentricity ratios, at the lower values of dimensionless supply pressure (0 and 0.5) a significant divergence became apparent at low eccentricity ratios ($\varepsilon < 0.5$). The major sources of experimental error were felt to be the introduction of shaft/

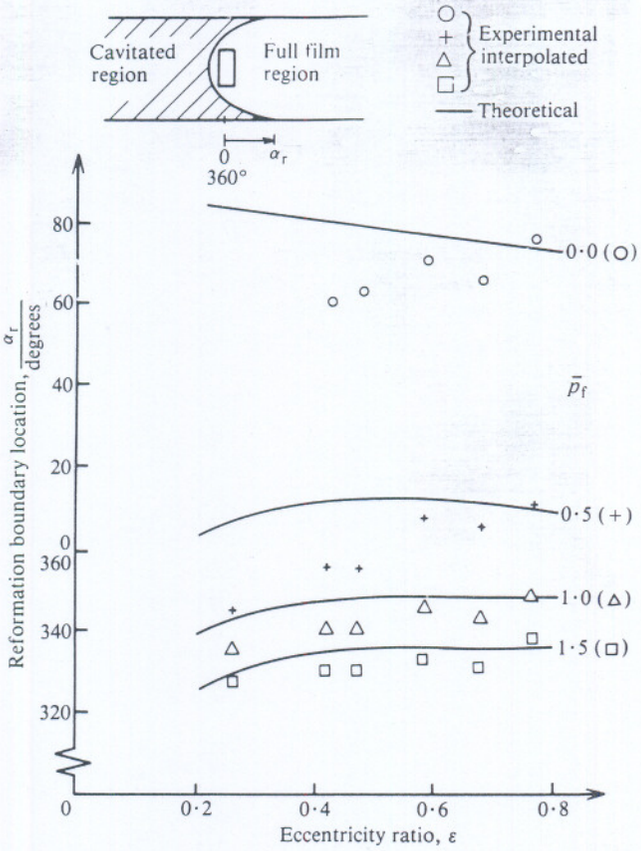

Fig. 9 A comparison of the interpolated experimental results for the location of the film reformation boundary with the theoretical predictions for *bush 2* (axial groove, $a/b = 0.409$). Shaft speed 600 r/min (10 Hz)

misalignment and imprecise location of the ... of maximum film thickness (**5**). However, it does not seem reasonable to attribute the discrepancies observed at low values of eccentricity ratio with low dimensionless supply pressure to these causes. It is worth noting that very good agreement between theoretical and experimental values of side leakage rate was obtained for such conditions. An explanation for the discrepancies reported has not yet been identified. The trend of the experimental data for $\bar{p}_f = 0$ is consistent with the predictions of Etsion and Pinkus (**9**). The authors believe, however, that the Etsion and Pinkus continuity condition at film reformation is incorrect (**1**).

A presentation of experimental data for the angular location of the rupture boundary, α_c is given in Fig. 10 for the tests carried out with bush 3 at a fixed shaft speed. The oil supply pressure did not significantly affect the location of this boundary which was essentially straight. The theoretical curve of Fig. 10 details the predictions of α_c for all values of $\bar{p}_f$ with a maximum error of 3.5°. Whilst the general trend of the experimental and theoretical results is good, large differences (between 30° to 42°) are obtained at all values of eccentricity ratio.

Such large discrepancies are attributed to the inadequacy of the film rupture model incorporated in the theoretical analysis. The application of the Elrod and Adams cavitation algorithm (**2**, **3**) invokes the Reynolds boundary condition at rupture (**1**). This denies the possibility of sub-ambient (or negative gauge) pressures in the film. The existence of a sub-ambient pressure region immediately upstream of the cavitation region has been observed by many research workers. Indeed the occurrence of tensile stresses in lubricant films has been experimentally confirmed. A detailed discussion of film rupture boundary conditions which might be appropriate, particularly for lightly loaded bearing situations, may be found in Dowson and Taylor (**10**). The works of Floberg (**11**, **12**), Coyne and Elrod (**13**, **14**) and Taylor (**15**) have clearly identified that alternative rupture boundary conditions to those identified by Reynolds may result in significant differences in the prediction of the location of the rupture boundary. This is seen as the undoubted source of the discrepancies apparent in Fig. 10 particularly since the discrepancy is in the direction to be expected if a sub-ambient pressure occurs immediately upstream of the rupture boundary. The inadequacy of the prediction of the location of the film rupture boundary does not appear to be significant in the determination of the lubricant side leakage flowrate. This is probably because the predicted flowrate across the rupture boundary is not greatly affected by the model adopted (**15**) and if this is the case the continuity considerations involved in specifying flow conditions at inlet will not be seriously influenced. Further, since the pressures in the vicinity of film rupture must necessarily be small, it would be expected that other characteristics (e.g. load capacity) would also not be greatly affected for moderately and heavily loaded bearing situations.

It is interesting to speculate that the differences between the theoretical and experimental data for reformation boundary location (Fig. 9) at low dimensionless supply pressure and low eccentricity ratio might be due to the error in predicting rupture boundary location.

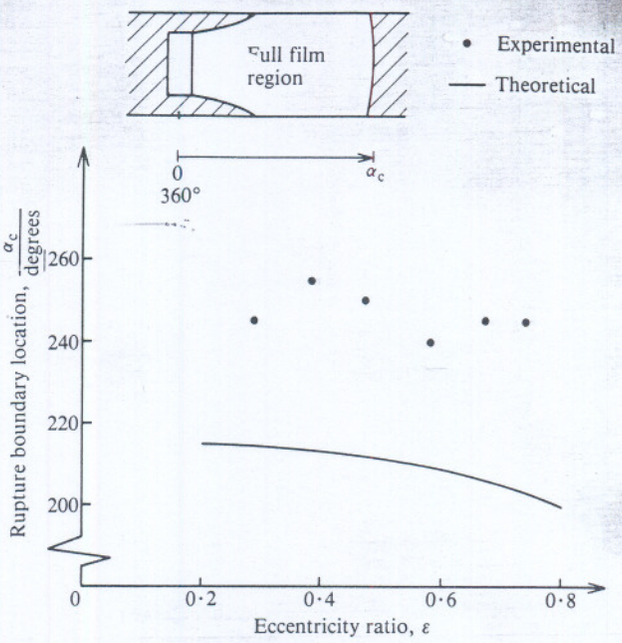

Fig. 10 A comparison of the experimental results for the location of the film rupture boundary with the theoretical predictions for *bush 3* (axial groove, $a/b = 0.708$) at all values of supply pressure. Shaft speed 600 r/min (10 Hz)

The influence of dimensionless supply pressure upon the location of the reformation boundary for a fixed eccentricity ratio ($\varepsilon = 0.7$) and shaft speed of 600 r/min for bush 1 is shown in Fig. 11. The correlation between theory and practice is again good, the maximum discrepancy being about 11° in α_r at $\bar{p}_f = 0.38$. The results shown in Fig. 11 are consistent with those for dimen-

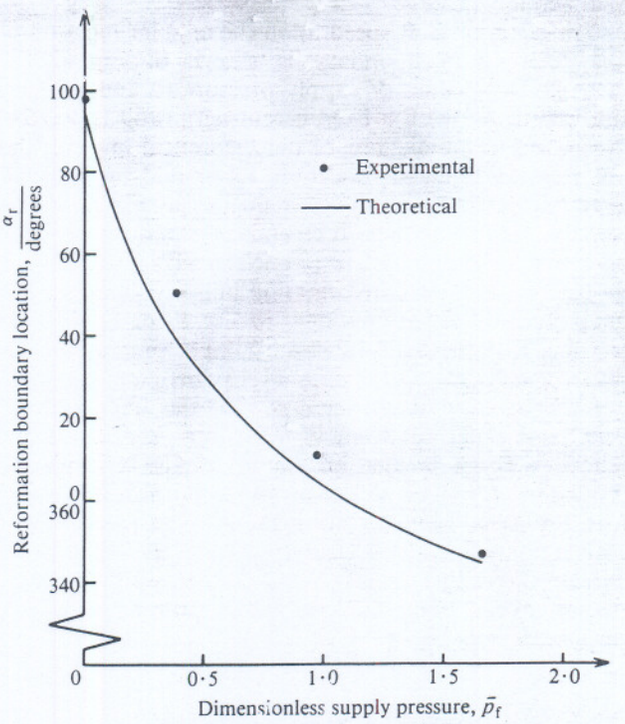

Fig. 11 The influence of dimensionless supply pressure on the location of the film reformation boundary for *bush 1* (oil hole). Shaft speed 600 r/min (10 Hz), eccentricity ratio $\varepsilon = 0.74$

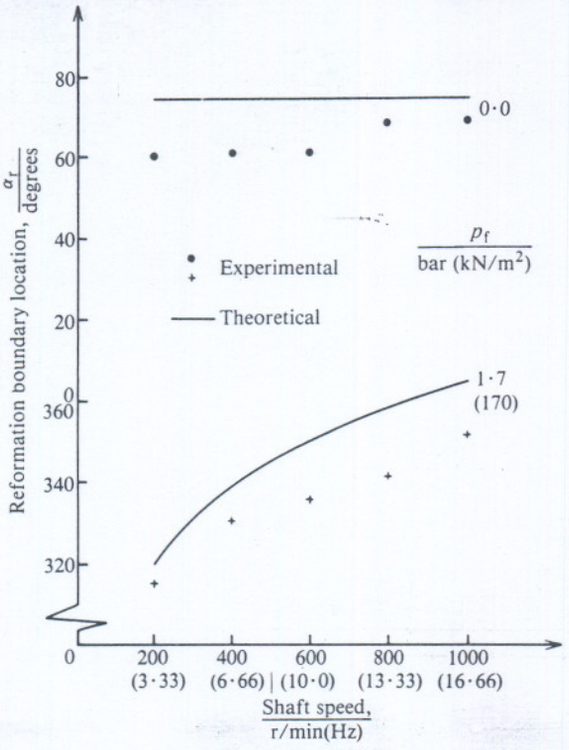

Fig. 12 The influence of shaft speed on the location of the film reformation boundary for *bush 2* (axial groove, $a/b = 0.409$). Eccentricity ratio $\varepsilon = 0.67$

sionless side leakage in Fig. 6 for the maximum value of eccentricity ratio tests ($\varepsilon = 0.75$). The theoretically predicted flowrate is always slightly larger than that measured experimentally. This in turn would correspond to a predicted reformation boundary location upstream of that actually observed.

The effect of shaft speed upon the angular location of the reformation boundary is shown in Fig. 12 for bush 2. Two values of supply pressure (0 and 1.7 bar) are considered with a fixed eccentricity ratio ($\varepsilon = 0.67$). According to predictions of the theoretical analysis the reformation boundary location, α_r, should be independent of the shaft rotational frequency at a zero gauge supply pressure for a fixed eccentricity ratio. The experimental results confirm this prediction with discrepancies in the location of the reformation boundary of a similar magnitude of those presented in Fig. 9 for $\bar{p}_f = 0$ and $\varepsilon > 0.5$. For the fixed lubricant supply pressure of 1.7 bar a maximum discrepancy of 16° between the theoretical and experimental values of α_r was obtained at a shaft rotational frequency of 800 r/min. At shaft speeds above 600 r/min the instability at the reformation boundary described earlier occurred and this influenced the empirical value for its location. The experimental values for reformation boundary location were all upstream of the theoretically predicted values. This is consistent overall with the correlation presented for side leakage flow in Fig. 8.

5 CONCLUSIONS

The authors have undertaken a programme of work studying the influence of lubricant film reformation in plain journal bearings. Earlier publications (1 and Part 1 of the present paper) have dealt with the implementation of a cavitation algorithm to locate both rupture and reformation boundaries in a computer analysis and the presentation of theoretical data generated using the algorithm. In the present paper an experimental investigation designed to establish the validity of the analysis has been reported.

1. The experimental programme has involved the testing of three bushes, all made of glass to facilitate visualization of the lubricant film. Bush 1 had an oil supply hole whilst the other bushes had a supply groove. In each case the oil supply to the bearing was located at the position of maximum film thickness.
2. A wide range of tests has been carried out using each bush and varying the eccentricity ratio, supply pressure and shaft rotational speed. The results presented have covered the lubricant side leakage rate and the location of the film reformation and rupture boundaries and their correlation with theoretically predicted data.
3. *Side leakage rate* The agreement between the experimentally determined lubricant side leakage and that predicted theoretically has been outstandingly good over the whole range of test variables covered. The excellent correlation obtained is particularly noteworthy since the differences between theoretical and experimental data for flowrate are commonly substantial. In the experiments carried out by the authors specific attention was paid to the design of the apparatus to ensure the utmost accuracy in the determination of the influential variables. In particular the design fixed the relative location of the shaft and bush, and hence the eccentricity ratio was known with precision. In tests where the eccentricity has to be measured with transducers, errors are easily introduced which can lead to poor correlation. In addition the minimization of shaft/bush misalignment was an important priority.

However, a good correlation is also dependent upon a well founded analytical model. The inclusion of a consideration of film reformation in the present analysis has been essential in obtaining the agreement. This is demonstrated in the following table:

	Predicted dimensionless side leakag	
	Flowrate for zero supply pressure wi an eccentricity ratio of 0.6	
Test bearing $b/d = 1$ $w/d = 0.189$	Current analysis with film reformation	Analysis takir full width filr at inlet
Bush 1 (oil hole, $a/b = 0.189$)	0.12	0.47
Bush 2 (supply groove, $a/b = 0.409$)	0.22	0.47
Bush 3 (supply groove, $a/b = 0.709$)	0.32	0.47

Clearly an analysis which only considered the rupture of the lubricant film with no consideration of inlet effects may be substantially in error in the prediction of side leakage flowrate. The use of such data in design will in turn lead to unacceptable estimates of important limiting operational criteria.

4. *Location of the film reformation boundary* The agreement between the observed and predicted film reformation boundary locations was good for eccentricity ratios of $\varepsilon > 0.6$. However, at low eccentricity ratio and low dimensionless supply pressure a significant difference was obtained, the experimental value of α_r being upstream of the predicted position.
5. *Location of the film rupture boundary* A large difference between the experimentally measured and theoretically predicted position of the film rupture boundary was obtained although the trend of the comparison was good. The discrepancy is attributed to the inadequate model of the rupture process which does not admit negative gauge pressures in the lubricant film.

REFERENCES

1 **Dowson, D., Miranda, A. A. S.** and **Taylor, C. M.** Implementation of an algorithm enabling the determination of film rupture and reformation boundaries in a liquid film bearing. *Proceedings of the 10th Leeds–Lyon Symposium on Tribology: developments in numerical and experimental methods applied to tribology*, 1984 (Butterworths).

2 **Elrod, H. G.** and **Adams, M. L.** A computer program for cavitation and starvation problems. *Proceedings of the 1st Leeds–Lyon Symposium on Tribology: cavitation and related phenomena in lubrication*, 1975, 37–42 (Mechanical Engineering Publications Limited, London).

3 **Elrod, H. G.** A cavitation algorithm. *Trans ASME, J. Lubric. Tech.* July 1981, **103,** 350–354.

4 *Calculation methods for steadily loaded pressure fed hydrodynamic journal bearings*, Engineering Sciences Data Unit (ESDU International Ltd). Item No. 66023, 1966.

5 **Miranda, A. A. S.** Oil flow, cavitation and film reformation in journal bearings including an interactive computer-aided design study. PhD Thesis, Dept of Mech. Engng, Univ. of Leeds, 1983.

6 **Cole, J. A.** and **Hughes, C. J.** Oil flow and film extent in complete journal bearings. *Proc. Instn Mech. Engrs*, 1956, **170,** 499.

7 **Hargreaves, D. J.** and **Taylor, C. M.** An experimental and theoretical study of lubricant film extent and flowrate in grooved rectangular pad slider thrust bearings. *Proc. Instn Mech. Engrs*, Part C, 1984, **198,** 225–233.

8 **Hargreaves, D. J.** and **Taylor, C. M.** An experimental and theoretical study of lubricant flowrate in static, grooved, rectangular thrust bearings. *J. Mech. Engng Sci.*, 1982, **24**(1), 51–54.

9 **Etsion, I.** and **Pinkus, O.** Solutions for finite journal bearings with new upstream boundary conditions. *Trans. ASME, J. Lubric. Tech.*, 1975, **97**(1).

10 **Dowson, D.** and **Taylor, C. M.** Cavitation in bearings. *Ann. Rev. Fluid Mechanics*, Vol. **11,** Annual Reviews, 1979.

11 **Floberg, L.** On hydrodynamic lubrication with special reference to sub-cavity pressures and number of streamers in cavitation regions. *Acta. Poly. Scand.*, Mech. Engng Series, ME19, 1965.

12 **Floberg, L.** Sub-cavity pressures and number of oil streamers in cavitation regions with special reference to the infinite journal bearing. *Acta. Poly. Scand.*, Mech. Engng Series, ME37, 1968.

13 **Coyne, J. C.** and **Elrod, H. G.** Conditions for the rupture of a lubricating film. Part I: theoretical model. *Trans. ASME, J. Lubric. Tech.*, 1970, **92**(3).

14 **Coyne, J. C.** and **Elrod, H. G.** Conditions for the rupture of a lubricating film. Part II: new boundary conditions for Reynolds' equation. *Trans ASME, J. Lubric. Tech.*, 1971, **93**(1).

15 **Taylor, C. M.** Separation cavitation: solutions for the infinite width cylinder-plane and journal bearing configurations. *J. Mech. Engng Sci.*, 1973, **15**(3), 237–239.